

# Injecting Electronic Excitation Energy into an Artificial Antenna System through an Ru<sup>2+</sup> Complex

Olivia Bossart,<sup>[a]</sup> Luisa De Cola,<sup>[b]</sup> Steve Welter,<sup>[b]</sup> and Gion Calzaferri\*<sup>[a]</sup>

**Abstract:** The Ru<sup>2+</sup> complex [Ru(bpy)<sub>2</sub>(bpy-ph<sub>4</sub>-Si(CH<sub>3</sub>)<sub>3</sub>)]<sup>2+</sup> can be electrostatically bound to the negatively charged channel entrances of dye-loaded zeolite L crystals where it acts as a functional stopcock molecule. Impressive electronic triplet–singlet excitation energy transfer from the Ru<sup>2+</sup> complex to the acceptor dye oxazine 1 (Ox1) located inside the channels can be observed when the donor molecule

is selectively excited. Time-resolved luminescence experiments have been performed on the separate components and on the assembled donor–acceptor material. The luminescence lifetime of the Ru<sup>2+</sup> complex attached to the zeo-

lite is reduced by a factor of 30 when Ox1 acceptor molecules are present. The fluorescence decay of Ox1 incorporated in zeolite L is single exponential with a lifetime of 3 ns. The much longer lifetime in zeolite L than in solution is due to the fact, that the diethyl groups are sterically restricted when the dye is inside the host.

**Keywords:** dyes/pigments • energy transfer • luminescence • ruthenium • supramolecular chemistry • zeolites

## Introduction

To collect light energy, transporting it from A to B with as little loss as possible and trapping it at a specific position, is a challenging goal researchers have in mind when they try to mimic the photosynthetic system of green plants.<sup>[1–4]</sup> Artificial photonic antenna materials that work well have been obtained by inserting fluorescent dye molecules into zeolite L crystals.<sup>[5]</sup>

Zeolite L is an aluminosilicate with one-dimensional channels running along the *c* axis of the hexagonal crystals.<sup>[6]</sup> Its stoichiometry with monovalent cations is (M)<sub>9</sub>[Al<sub>9</sub>Si<sub>27</sub>O<sub>72</sub>]*n*H<sub>2</sub>O, where *n* equals 21 in fully hydrated materials and 16 at about 20% relative humidity. The number of channels in a zeolite L crystal of diameter *d<sub>c</sub>* given in nm is equal to 0.265(*d<sub>c</sub>*)<sup>2</sup>. As an example, a crystal with a diameter of 550 nm consists of about 80000 parallel channels. They can be subdivided into unit cells of 0.75 nm length. Hence, zeolite crystals of 500 nm in length and diameter consist of 44 × 10<sup>6</sup> unit cells. The channels have an opening diameter of 0.71 nm and a distance of 1.84 nm. Only dyes that can pass

the 0.71 nm opening are able to enter the crystals, in which they are positioned at sites along the linear channels. A site *s* is defined by the number of unit cells one dye molecule covers and therefore depends on the size of the inserted dye. The length of a site corresponds to a number *s* times the unit cell length, so that one dye molecule fits into one site. The occupation probability *p* is equal to the ratio of the occupied sites to the total number of sites. Hence, the dye concentration *c*(*p*) in mol L<sup>-1</sup> in a dye loaded zeolite L crystal is related to the occupation probability *p* by Equation (1) in which  $\rho_z$  is the density of the crystal, *M<sub>r</sub>* is the molar mass of the unit cell, and *s* is the number of unit cells needed for one site.

$$c(p) = \frac{\rho_z p}{M_r s} \quad (1)$$

Inserting the values for zeolite L ( $\rho_z = 2.17 \text{ g cm}^{-3}$ ; *M<sub>r</sub>* = 2883 g mol<sup>-1</sup>) and an *s* value of 2 (corresponds to oxazine 1) we obtain Equation (2). We refer to reference [5] for further details.

$$c(p) = (0.376 \text{ mol L}^{-1})p \quad (2)$$

Due to these one-dimensional channels, zeolite L is an ideal host material. Dyes of appropriate shape can enter its channels, but once inside they are prevented from forming dimers due to spatial restrictions. Hence, highly anisotropic materials with a very large dye concentration can be built. This is a prerequisite for observing efficient electronic exci-

[a] Dipl.-Chem. O. Bossart, Prof. Dr. G. Calzaferri  
Department of Chemistry and Biochemistry  
University of Berne, 3012 Berne (Switzerland)  
Fax: (+41)31-631-3994  
E-mail: gion.calzaferri@iac.unibe.ch

[b] Prof. Dr. L. De Cola, MSc. S. Welter  
University of Amsterdam, Nieuwe Achtergracht  
166, 1018 WV Amsterdam (The Netherlands)

tation energy transfer.<sup>[7]</sup>

We have reported photonic antenna materials with two and three different types of dyes, in which the donors are either located in the middle of the zeolite L channels and the acceptors at the ends or vice versa.<sup>[5,8,9]</sup> Using functional stopcock molecules, we have synthesized systems in which the excitation energy running through the channels can be collected on the outside of the crystals or be injected into them (Figure 1), depending on the arrangement.<sup>[10,11]</sup> In this research, so far only organic dye molecules have been used, in which singlet–singlet Förster type energy transfer was observed [Eq. (3); D = donor, A = acceptor].



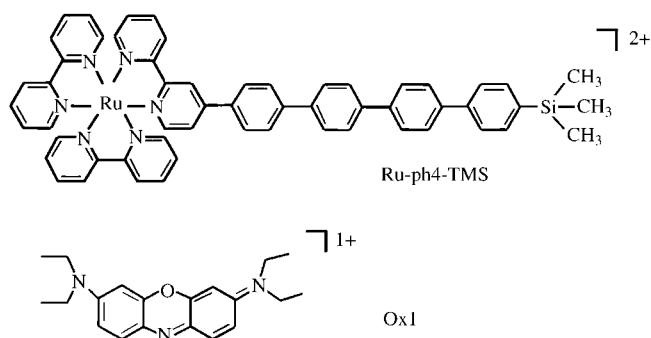
We now report experiments with a luminescent  $\text{Ru}^{2+}$  complex acting as a functional stopcock molecule. It consists of a head, which is too large to enter the 7.1 Å wide entrances of zeolite L, and a tail that can penetrate into the channels. The stopcocks are electrostatically bound to the negatively charged channel entrances; this gives the system a high stability. We will show that very efficient triplet–singlet energy transfer takes place [Eq. (4)], leading to injection of electronic excitation energy into the dye-loaded crystals, when selectively exciting the stopcock, as illustrated in Figure 1a.



## Results and Discussion

Experiments were carried out with zeolite crystals ranging from 30 nm up to 5000 nm in length. The large crystals allow characterization by means of optical luminescence microscopy, while the small ones are interesting for incorporation into a device. Throughout this manuscript the stopcock complex  $[\text{Ru}(\text{bpy})_2(\text{bpy-ph}_4\text{-Si}(\text{CH}_3)_3)]^{2+}$  will be abbreviated as Ru-ph4-TMS and the strongly luminescent acceptor molecule oxazine 1 as Ox1.

**Donor:** Ru-ph4-TMS is a suitable stopcock molecule. Its organic tail fits nicely into the zeolite L channels, whereas its head is too large to enter. Furthermore its photophysical properties make it an ideal excitation energy donor. It is



highly luminescent, its excited state is long lived, and it possesses different absorption bands at different energies, allowing selective excitation in the presence of an acceptor molecule. The host material zeolite L can be subdivided into two areas with distinctly different chemical properties: the flat base containing the channel openings and the vaulted coat. When one Ru-ph4-TMS per channel is added to zeolite L, it is selectively adsorbed to the negatively charged channel openings, where it is electrostatically bound as illustrated in Figure 1. The fluorescence microscopy images in Figure 2 show a 5000 nm long crystal modified with one

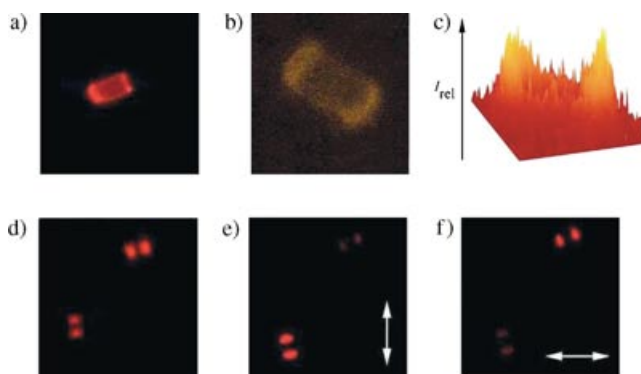


Figure 2. Fluorescence microscopy images of 5000 nm long crystals. Top: Crystal modified with one Ru-ph4-TMS per channel: a) conventional and b) confocal microscopy images indicate that the Ru-ph4-TMS stopcocks are selectively adsorbed at the channel ends. c) The luminescence intensity distribution of b). Bottom: Ox1 loaded crystals. The microscopy image d) shows two crystals lying almost at right angles. Polarized images in e) and f) of the same crystals show their anisotropic properties. The direction of the transmitted light is indicated by the double arrows.

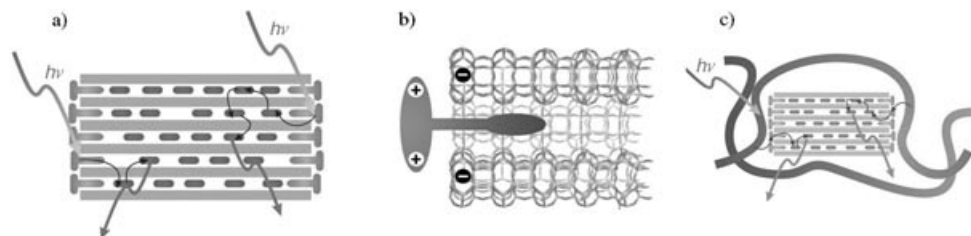


Figure 1. Artificial antenna system. a) Representation of a cylindrical nanocrystal containing luminescent dye molecules (shaded rectangles) and functional stopcock molecules closing the channels (shaded T-shaped bars). Electronic excitation energy absorbed by the stopcocks can be transferred to the dyes located inside the channels. b) Scheme of a functional stopcock molecule which is electrostatically bound to the entrance of a channel. c) Incorporation of an antenna into a fluorescent polymer leads to interesting new materials, for example, LED devices.

Ru-ph4-TMS per channel. The Ru-ph4-TMS molecule was excited from 320 nm to 385 nm and the fluorescence was detected with a 420 nm cut off filter (Figure 2a). The images in Figures 2b and 2c were taken in confocal mode by exciting the Ru-ph4-TMS by means of an Argon laser at 488 nm and detecting the emitted light through a 510 nm cut off filter. Figure 2c shows the relative intensity ( $I_{\text{rel}}$ ) of the emission in a three-dimensional plot.

**Acceptor:** Ox1 was found to be an ideal acceptor for electronic excitation energy transfer from Ru-ph4-TMS. Its fluorescent excited state is lower in energy than the  $^3\text{MLCT}$  excited state of the ruthenium complex. A difficulty encountered was that this cationic dye cannot be inserted by “standard” ion-exchange conditions from water, because of the dimethylamino groups. We found that it can be inserted from a suspension in toluene upon heating. Once inside the channels, Ox1 is aligned parallel to the channels so that a very stable, strongly luminescent and optically highly anisotropic material is obtained as illustrated in Figure 2d–f. The Ox1 molecules are located near the channel ends in these crystals. Their slow diffusion at room temperature inside the channels makes it possible to prepare such samples.

**Coupled system—second stage of organization:**<sup>[5]</sup> A prerequisite for observing Förster type energy transfer is a large spectral overlap between the absorption and the emission spectra of the acceptor and the donor, respectively. Furthermore, it must be possible to selectively excite the donor. The use of Ru-ph4-TMS as a donor and Ox1 as an acceptor meets these conditions perfectly (Figure 3). The Förster radius, at which 50% of the energy is transferred, is 10 nm (spectral overlap  $1.0 \times 10^{-9} \text{ cm}^6 \text{ mol}^{-1}$ ), which is unusually large.<sup>[12,13]</sup> For the following experiments zeolite L crystals of 500 nm in length and diameter were used. The overall occupation probability of Ox1 was chosen to be  $p = 0.006$ . This corresponds, according to Equation (2), to a mean concentration of  $2.3 \times 10^{-3} \text{ mol L}^{-1}$ . This concentration would be too low for the experiments envisaged here. However, the short insertion time of the Ox1 molecules does not allow them to diffuse far into the channels, so that the local concentration at both ends of the channels is much higher. Hence, on average one Ox1 molecule is located close to the channel ends. These conditions were used in order to minimize direct excitation of the acceptors at the excitation wavelengths so that it can be neglected. When these crystals are modified with one molecule of Ru-ph4-TMS per channel, approximately a 2:1 acceptor to donor ratio is present. The Ru-ph4-TMS complex can be excited in its  $^1\text{MLCT}$  band at 460 nm, at which Ox1 exhibits a negligible absorption under the given conditions. The data in Figure 3 illustrate that the Ru-ph4-TMS  $\rightarrow$  Ox1 energy transfer is indeed very efficient, even though the donor and acceptor moieties are not covalently linked. The emission of the ruthenium complex upon excitation at 460 nm almost completely vanishes and is only present as a shoulder at 610 nm, while sensitization of the Ox1 is achieved as demonstrated by the intense emission at 670 nm, Figure 3b. The same behavior was observed when 30 nm long crystals were loaded with an acceptor to donor

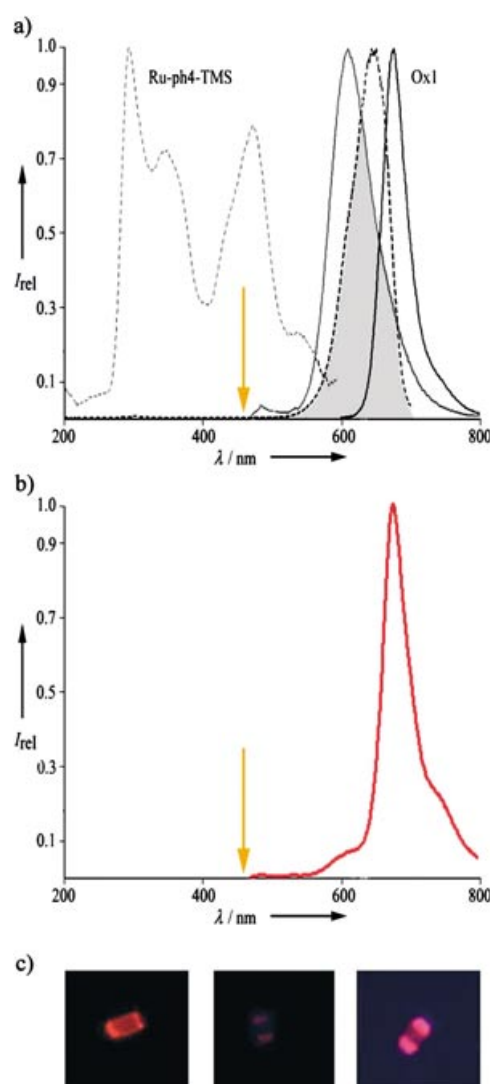


Figure 3. a) Excitation (dashed) and emission (solid) spectra of Ru-ph4-TMS at the channel ends and of Ox1 inside. The spectral overlap region is shaded. At 460 nm (arrow) Ru-ph4-TMS can be selectively excited. b) Emission spectrum of Ox1 loaded zeolite ( $p = 0.006$ ) modified with one Ru-ph4-TMS per channel, observed after excitation at 460 nm. The shoulder at 610 nm is the remaining weak emission of Ru-ph4-TMS. The large peak at 670 nm is the sensitized emission of Ox1. c) Fluorescence microscopy images of crystals loaded with one Ru-ph4-TMS per channel (left), with Ox1 (middle) and with both (right). The three images were recorded upon selective excitation of Ru-ph4-TMS.

ratio of 2:1. We note that irradiation of an isoabsorptive sample at 460 nm containing only the Ox1 leads to almost no emission.

Time-resolved luminescence experiments have been performed on the separate components and on the assembled donor–acceptor system with 500 nm long crystals at room temperature. The data are reported in Table 1.

The Ru-ph4-TMS complex at the channel ends shows a biexponential luminescence decay with an average lifetime  $\bar{\tau}$  of 580 ns [Eq. (5)].

$$\bar{\tau} = \frac{a_1\tau_1^2 + a_2\tau_2^2}{a_1\tau_1 + a_2\tau_2} \quad (5)$$

Table 1. Wavelengths of excitation  $\lambda_{\text{ex}}$  and detection  $\lambda_{\text{det}}$ , luminescence decay time  $\tau$ , their relative weights  $a$  ( $a_1$  and  $a_2$ ) and the mean luminescence decay time  $\bar{\tau}$  of the separate components and of the assembled donor–acceptor system.

Sample	$\lambda_{\text{ex}}$ [nm]	$\lambda_{\text{det}}$ [nm]	$\tau$ [ns]	$\bar{\tau}$ [ns]	$a$
zeolite with Ru-ph4-TMS	450	450–700	610 110	576	0.71 0.29
zeolite with Ox1	620	700	3.0		
zeolite with Ru-ph4-TMS and Ox1	465	690	3.0 1.2 19	2.6	0.51 0.42 0.07

The fluorescence decay of Ox1 incorporated in zeolite L is single exponential with a lifetime of 3 ns. In solution at room temperature, its lifetime ranges from 0.5 to 1.3 ns, depending on the solvent.<sup>[14]</sup> The up to six times longer lifetime in zeolite L is due to the fact that the diethyl groups are sterically restricted when the dye is inside of the host, thus blocking fast, radiationless decay channels.<sup>[15]</sup> The coupled system shows a triple exponential decay. The long-lifetime component can be assigned to the decay of the donor and the two shorter ones to the acceptor. The average fluorescence lifetime of the acceptor is 2.6 ns. The luminescence lifetime of Ru-ph4-TMS is reduced from 580 to 19 ns, which is a factor of 30, when acceptor molecules are present, while the rise of the Ox1 fluorescence was not observed. This underlines the efficient and fast Ru-ph4-TMS to Ox1 energy transfer.

## Conclusion

The use of the Ru-ph4-TMS complex as a functional stopcock molecule results in an impressive electronic excitation energy transfer to the acceptor dye unit inside the zeolite channels. The efficiency of the process for a noncovalent dyad based on a ruthenium complex as donor and organic dyes as acceptor is astonishingly high. In covalently linked systems in which the donor (ruthenium unit) and acceptor (osmium unit) are separated by five tilted phenylene units the efficiency of energy transfer was comparable.<sup>[16]</sup> The system works with crystals ranging from 30 nm in length and diameter to crystals of 5000 nm in length and 3000 nm in diameter; this is equal to a change in volume by a factor of  $10^6$ . The properties of this host–guest material differ strongly from covalently linked donor–acceptor energy-transfer systems.<sup>[1,16]</sup> Our results are expected to advance a wide range of applications, some of which we have recently discussed.<sup>[5]</sup>

## Experimental Section

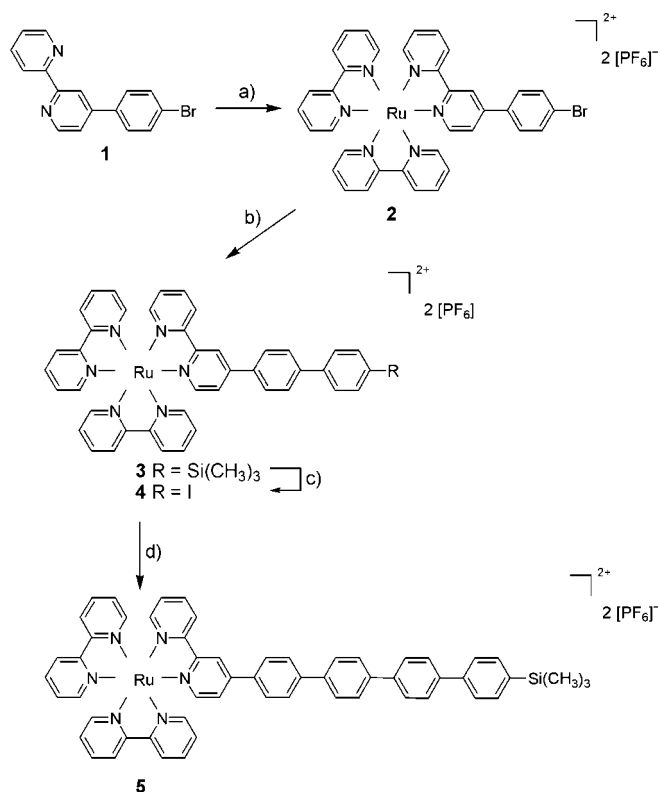
**Zeolite L:** Zeolite L material was synthesized and characterized as described in reference [8]. The potassium-exchanged form of the crystals was used. For luminescence and confocal microscopy images, crystals of 5000 nm in length and 3000 nm in diameter were used, while the energy transfer experiments were conducted with crystals of 30 nm and 500 nm in size. Laser grade Ox1 was used without further purification. Ox1 was

inserted into the zeolite L channels by ion exchange out of toluene. Typically zeolite L (20 mg) was suspended in toluene (5 mL). The suspension was stirred vigorously while the desired amount of Ox1 suspended in toluene (100  $\mu\text{L}$ ) was added. The mixture was heated to 80 °C for a few minutes. To remove any dye molecules adsorbed on the outer surface of the zeolite, the crystals were then washed with diluted Genapol X-080 from Fluka. Typically a watery Genapol X-080 solution (1:500; 5 mL) was added and the resulting suspension was sonicated for 10 min. It was then centrifuged until the supernatant was clear and could be discarded. For the adsorption of the Ru-ph4-TMS to the channel ends, typically zeolite crystals (10 mg) were suspended in  $\text{CH}_2\text{Cl}_2$  (3 mL). A solution containing the amount of Ru-ph4-TMS corresponding to one molecule per channel in  $\text{CH}_2\text{Cl}_2$  (100  $\mu\text{L}$ ) was added, and the suspension was sonicated for 15 min at room temperature. Best results were obtained when the crystals were then kept in  $\text{CH}_2\text{Cl}_2$  at room temperature for one week.

**Luminescence spectra:** Luminescence spectra of samples (6 mg) suspended in  $\text{CH}_2\text{Cl}_2$  (3 mL) were measured with a Perkin–Elmer LS 50B instrument. Time-resolved measurements of the Ox1 loaded crystals and of the coupled system were conducted as described in reference [17]. Layers of the samples were prepared on quartz plates. The samples were flushed with  $\text{N}_2$  during the measurements. The zeolite crystals modified with Ru-ph4-TMS were measured in a  $\text{CH}_2\text{Cl}_2$  suspension. For the luminescence microscopic images an Olympus BX60 microscope equipped with a Kappa CF20DCX air-cooled CCD camera was used. The Ru-ph4-TMS complex was excited from 320 to 385 nm and the fluorescence was detected by using a 420 nm cut off filter. Ox1 was excited from 590 nm to 650 nm and the emission was detected by using a cut off filter at 665 nm. The confocal microscopy images were obtained with a fluoview FV300 accessory equipped with an argon laser operating at 488 nm and a HeNe laser at 543.5 nm. The microscopy images were made of single crystals on a glass support exposed to air.

### Synthesis of Ru-ph4-TMS

**General:** The synthesis of Ru-ph4-TMS was carried out as described below, Scheme 1. Reagents and solvents were all commercially available



Scheme 1. a) [Ru(bpy)<sub>2</sub>Cl<sub>2</sub>], ethylene glycol, microwave irradiation; b) 4-trimethylsilylphenylboronic acid, K<sub>2</sub>CO<sub>3</sub>, [Pd(PPh<sub>3</sub>)<sub>4</sub>], DMF, 95 °C, 15 h; c) ICl, CH<sub>2</sub>Cl<sub>2</sub>; d) 4'-trimethylsilylbiphenyl-4-boronic acid, K<sub>2</sub>CO<sub>3</sub>, [Pd(PPh<sub>3</sub>)<sub>4</sub>], DMF, 95 °C, 15 h.<sup>[18]</sup>

and used as received.  $[\text{Ru}(\text{bpy})_2\text{Cl}_2]$ ,<sup>[19]</sup> 4'-trimethylsilylbiphenyl-4-boronic acid,<sup>[20]</sup> and the ligand 4-(4-bromophenyl)-[2,2']bipyridine (**1**),<sup>[21]</sup> were prepared following literature procedures. All experiments were carried out under  $\text{N}_2$  atmosphere using standard Schlenk tube techniques. Chromatographic purification was conducted by using 40–63  $\mu\text{m}$  silica gel purchased from FLUKA. Thin-layer chromatography (TLC) on silica gel was performed with  $\text{CH}_3\text{CN}/\text{H}_2\text{O}/\text{CH}_3\text{OH}/\text{NaCl}$  (4:1:1:0.1) as eluent for all the ruthenium complexes. NMR spectra were recorded on a Varian Mercury-VX (300 MHz) by using the residual nondeuterated solvent as reference. Electron spray ionization (ESI) mass spectra were measured with a Bruker FTMS 4.7 T Bio APEXII spectrometer. Further details are reported in reference [18].

**[Ru(bpy)<sub>2</sub>(bpy-ph-Br)]<sup>2+</sup>(PF<sub>6</sub>)<sub>2</sub> (2):**  $[\text{Ru}(\text{bpy})_2\text{Cl}_2]$  (110.7 mg, 0.21 mmol) and **1** (50.6 mg, 0.16 mmol) were dissolved in ethylene glycol (5 mL). The mixture was placed in a modified microwave oven and irradiated at 450 Watt for 2 min and, after a cooling down period, for another 2 minutes. The stage of conversion was checked by TLC (silica,  $\text{MeCN}/\text{H}_2\text{O}/\text{MeOH}/\text{KNO}_3$ , 4:1:1:0.1) and the reaction mixture was further irradiated if necessary. The solvent was distilled under vacuum by using a "micro distillation head" at high temperature (90–110 °C). The dark red compound was dissolved in water (20 mL) and the water phase was extracted with chloroform to remove the excess  $[\text{Ru}(\text{bpy})_2\text{Cl}_2]$ . The remaining chloroform and water phases were evaporated and the compound was purified by column chromatography on silica gel using  $\text{MeCN}/\text{H}_2\text{O}/\text{MeOH}/\text{NaCl}$ , 4:1:1:0.1 as eluent. The desired compound was collected and the organic solvents were evaporated.  $\text{NH}_4\text{PF}_6$  (1 g) in water (2 mL) was added to the remaining water layer to obtain an orange-red precipitate. The precipitate was filtered over Celite and washed several times with water. Finally the compound was eluted from Celite with acetone. Compound **2** was obtained as an orange powder with 81% yield (172 mg). <sup>1</sup>H NMR (300 MHz,  $\text{CD}_3\text{CN}$ , 25 °C):  $\delta$  = 8.71 (s, 1H), 8.68 (d,  $J$  = 8.0 Hz, 1H), 8.52 (dd,  $J$  = 8.3 Hz, 2.0 Hz, 4H), 8.06 (m, 5H), 7.82–7.70 (m, 10H), 7.62 (dd,  $J$  = 6 Hz, 1.8 Hz, 1H), 7.41 ppm (m, 5H); MS ESI:  $m/z$  (%): 869.02 (15)  $[\text{M}^+ - \text{PF}_6^-]$ , 363.03 (100)  $[\text{M}^+ - 2\text{PF}_6^-]$ .

**[Ru(bpy)<sub>2</sub>(bpy-ph<sub>2</sub>-Si(CH<sub>3</sub>)<sub>3</sub>)]<sup>2+</sup>(PF<sub>6</sub>)<sub>2</sub> (3):** In a Schlenk flask compound **2** (250 mg, 0.25 mmol), 4'-trimethylsilylbiphenylboronic acid (190 mg, 0.99 mmol), and potassium carbonate (136 mg, 0.99 mmol) were dissolved in *N,N*-dimethylformamide (25 mL). The solution was degassed three times using pump-freeze-thaw technique. Finally  $[\text{Pd}(\text{PPh}_3)_4]$  (14 mg, 0.01 mmol) was added, and the mixture was heated at 95 °C for 15 h. The solvent was removed under vacuum and the product was purified by column chromatography on silica gel using  $\text{MeCN}/\text{H}_2\text{O}/\text{MeOH}/\text{NaCl}$ , 4:1:1:0.1 as eluent. The fraction containing the pure complex was evaporated to dryness to yield an orange solid (243 mg, 91%). <sup>1</sup>H NMR (300 MHz,  $\text{CD}_3\text{CN}$ , 25 °C):  $\delta$  = 8.78 (d,  $J$  = 1.5 Hz, 1H), 8.70 (d,  $J$  = 8.0 Hz, 1H), 8.51 (dd,  $J$  = 8.3 Hz, 5.0 Hz, 4H), 8.06 (m, 5H), 7.73 (dd,  $J$  = 28.7 Hz, 8 Hz, 4H), 7.81–7.60 (m, 11H), 7.40 (m,  $J$  = 6 Hz, 5H), 0.33 ppm (s, 9H); MS ESI:  $m/z$  (%): 887.11 (15)  $[\text{M}^+ - \text{PF}_6^-]$ , 371.06 (100)  $[\text{M}^+ - 2\text{PF}_6^-]$ .

**[Ru(bpy)<sub>2</sub>(bpy-ph<sub>2</sub>-I)]<sup>2+</sup>(PF<sub>6</sub>)<sub>2</sub> (4):** Compound **3** (103 mg, 0.95 mmol) was dissolved in dichloromethane (10 mL), and the solution was cooled down to 0 °C. A solution of iodine chloride (0.23 g, 1.4 mmol) in dichloromethane (2 mL) was added slowly. After 1 h the ice-bath was removed and the solution was stirred for 1.5 h at room temperature. An aqueous solution of sodium metabisulfite (10 mL, 1 M) was added to quench the reaction, and the reaction mixture was extracted with dichloromethane. The organic layers were washed with water. After evaporation of the solvent a red solid was obtained (106 mg, 98%). <sup>1</sup>H NMR (300 MHz,  $\text{CD}_3\text{CN}$ , 25 °C):  $\delta$  = 8.77 (d,  $J$  = 1.5 Hz, 1H), 8.70 (d,  $J$  = 8.0 Hz, 1H), 8.51 (dd,  $J$  = 8.3 Hz, 5.0 Hz, 4H), 8.08–7.91 (m, 7H), 7.79–7.63 (m, 13H), 7.40 ppm (m, 5H); MS ESI:  $m/z$  (%): 992.98 (10)  $[\text{M}^+ - \text{PF}_6^-]$ , 423.99 (100)  $[\text{M}^+ - 2\text{PF}_6^-]$ .

**[Ru(bpy)<sub>2</sub>(bpy-ph<sub>4</sub>-Si(CH<sub>3</sub>)<sub>3</sub>)]<sup>2+</sup>(PF<sub>6</sub>)<sub>2</sub> (5):** In a Schlenk flask compound **4** (125 mg, 0.11 mmol), 4'-trimethylsilylbiphenyl-4-boronic acid (60 mg, 0.22 mmol), and potassium carbonate (90 mg, 0.66 mmol) were dissolved in *N,N*-dimethylformamide (20 mL). The solution was degassed three times by using a pump-freeze-thaw technique. Finally  $[\text{Pd}(\text{PPh}_3)_4]$  (12 mg, 0.01 mmol) was added and the mixture was heated at 95 °C for 15 h.

After purification, as described above for **3**, complex **5** was obtained as orange powder (125 mg, 92%). <sup>1</sup>H NMR (300 MHz,  $\text{CD}_3\text{CN}$ , 25 °C):  $\delta$  = 8.89 (d,  $J$  = 1.5 Hz, 1H), 8.81 (d,  $J$  = 8.1 Hz, 1H), 8.59 (t,  $J$  = 6.8 Hz, 4H), 8.15–8.05 (m, 6H), 7.97 (d,  $J$  = 8.4 Hz, 2H), 7.91–7.68 (m, 20H), 7.47–7.42 ppm (m, 5H); MS: ESI,  $m/z$  (%): 1091.31 (6)  $[\text{M}^+ - \text{PF}_6^-]$ , 473.15 (100)  $[\text{M}^+ - 2\text{PF}_6^-]$ .

## Acknowledgement

This work was supported by the Swiss National Science Foundation NFP 47 (4047-057481). We thank Arantzazu Zabala Ruiz and René Bühler for the synthesis of the 5000 nm and the 30 nm long zeolite L crystals, respectively, and Katsiaryna Lutkouskaya for performing time-resolved measurements.

- [1] a) V. Balzani, M. Venturi, A. Credi, *Molecular Devices and Machines. A Journey into the Nanoworld*, Wiley-VCH, Weinheim, **2003**; b) V. Balzani, S. Campagna, G. Denti, A. Juris, S. Serroni, M. Venturi, *Acc. Chem. Res.* **1998**, *31*, 26; c) L. Jullien, J. Canceill, B. Valeur, E. Bardez, J.-M. Lehn, *Angew. Chem.* **1994**, *106*, 2582; *Angew. Chem. Int. Ed.* **1994**, *33*, 2438.
- [2] D. Gust, T. A. Moore, A. L. Moore, *Pure Appl. Chem.* **1998**, *70*, 2189.
- [3] H. Bücher, K. H. Drexhage, M. Fleck, H. Kuhn, D. Möbius, F. P. Schäfer, J. Sondermann, W. Sperling, P. Tillmann, J. Wiegand, *Mol. Cryst.* **1967**, *2*, 199.
- [4] S. E. Webber, *Chem. Rev.* **1990**, *90*, 1469.
- [5] a) G. Calzaferri, S. Huber, H. Maas, C. Minkowski, *Angew. Chem.* **2003**, *115*, 3860; *Angew. Chem. Int. Ed.* **2003**, *42*, 3732; b) G. Calzaferri, H. Maas, M. Pauchard, M. Pfenniger, S. Megelski, A. Devaux, in *Advances in Photochemistry*, Vol. 27 (Eds.: D. C. Neckers, G. von Bünau, W. S. Jenks), Wiley, **2002**, p. 1; c) G. Calzaferri, M. Pauchard, H. Maas, S. Huber, A. Khatyr, T. Schaafsma, *J. Mater. Chem.* **2002**, *12*, 1.
- [6] C. Bärlocher, W. M. Meier, D. H. Olsen, *Atlas of Zeolite Framework Types*, Elsevier, Amsterdam, **2001**.
- [7] T. Förster, *Ann. Phys.* **1948**, *6*, 55.
- [8] S. Megelski, G. Calzaferri, *Adv. Funct. Mater.* **2001**, *11*, 277.
- [9] a) A. Devaux, C. Minkowski, G. Calzaferri, *Chem. Eur. J.* **2004**, *10*, 2391; b) M. Pauchard, A. Devaux, G. Calzaferri, *Chem. Eur. J.* **2000**, *6*, 3456.
- [10] H. Maas, G. Calzaferri, *Angew. Chem.* **2002**, *114*, 2389; *Angew. Chem. Int. Ed.* **2002**, *41*, 2284.
- [11] a) S. Huber, G. Calzaferri, *ChemPhysChem* **2004**, *5*, 239; b) H. Maas, G. Calzaferri, *The Spectrum* **2003**, *16*, 18.
- [12] D. L. Andrews, A. A. Demidov, *Resonance Energy Transfer*, Wiley, Chichester, West Sussex (UK), **1999**.
- [13] J. R. Lakowicz, *Principles of Fluorescence Spectroscopy*, 2nd ed., Kluwer Academic/Plenum, New York, **1999**.
- [14] S. Landgraf, G. Grampp, *Monatsh. Chem.* **2000**, *131*, 839.
- [15] S. Bergamasco, G. Calzaferri, K. Hädener, *J. Photochem. Photobiol. A* **1990**, *53*, 109.
- [16] B. Schlicke, P. Belser, L. De Cola, E. Sabbioni, V. Balzani *J. Am. Chem. Soc.* **1999**, *121*, 4207.
- [17] M. M. Yatskou, M. Meyer, S. Huber, M. Pfenniger, G. Calzaferri, *ChemPhysChem* **2003**, *4*, 567.
- [18] S. Welter, A. Benetti, N. Salluce, P. Belser, K. Muellen, L. De Cola, unpublished results.
- [19] B. P. Sullivan, D. J. Salmon, T. J. Meyer, *Inorg. Chem.* **1978**, *17*, 3334.
- [20] V. Hensel, A.-D. Schlüter, *Liebigs Ann./Recl.* **1997**, 303.
- [21] M. Querol, B. Bozic, N. Salluce, P. Belser, *Polyhedron* **2003**, *22*, 655.

Received: July 19, 2004  
Published online: October 7, 2004